

# REVOLUTIONIZING POWER TRANSFORMER FAULT DIAGNOSIS THROUGH COGNITIVE ARTIFICIAL INTELLIGENCE AND DISSOLVED GAS ANALYSIS INTEGRATION

Phoumsavath Souvannalath<sup>a\*</sup>, Suttichai Premrudeepreechacharn<sup>a</sup>, Kanchit Ngamsanroaj<sup>b</sup>

<sup>a</sup>Department of Electrical Engineering, Faculty of Engineering, Chiang Mai University (CMU), 50200, Chiang Mai, Thailand

<sup>b</sup>Electricity Generating Authority of Thailand, Nonthaburi, Thailand

## Article history

Received

22 November 2022

Received in revised form

11 September 2023

Accepted

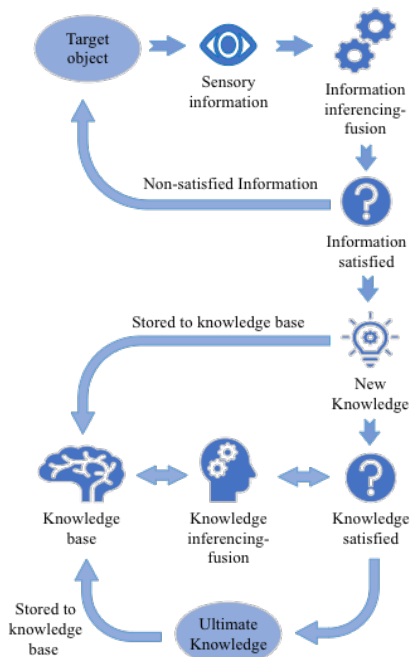
23 September 2023

Published online

31 August 2024

\*Corresponding author  
Phoumsavath\_s@cmu.ac.th

## Graphical abstract



## Abstract

The research introduces a cognitive artificial intelligence (CAI) model that leverages dissolved gas analysis (DGA) to investigate power transformer faults. Conventional fault interpretation methods using DGA are limited in accuracy and uncertainty. In response, the proposed CAI model utilizes cognitive learning and direct interaction to achieve remarkably accurate fault identification without the need for supervised training. By extracting fault features through key gas ratio limitations. However, the CAI model also has a gap in data perception due to the information sensory challenges. Using gas ratios based on the conventional fault interpretation methods in the latest study still limited data perception of the CAI model to only three or four gas ratios. Thus, this study aims to increase data perception by extracting fault features through ten gas ratio limitations. The proposed CAI model's performance is validated, outperforming traditional methods like the Duval triangle method, Duval pentagon method, Doernenburg ratio method, and Roger ratio method, as well as common AI approaches including artificial neuron network, long short-term memory, nearest neighbor classifiers, support vector machine, ensemble classifiers, and decision trees. Notably, the CAI model's success rate in fault type identification stands at an impressive 98.04%. A distinctive trait of the CAI model is its autonomous knowledge accumulation and enhancement, enabled by inferring-fusion information and sensor-based knowledge integration. This intrinsic learning ability further contributes to its exceptional fault diagnosis accuracy. The proposed CAI model showcases promising potential for revolutionizing power transformer fault investigation and diagnosis, mitigating unplanned outages, and ultimately bolstering power system reliability.

**Keywords:** Power transformer diagnosis, Cognitive artificial intelligence, Dissolved gas analysis

© 2024 Penerbit UTM Press. All rights reserved

## 1.0 INTRODUCTION

Power transformers are the key components of both the transmission and distribution power systems, which play an essential role in continuously operating to transfer power energy in the system. A power transformer failure typically results in a major power outage, resulting in insufficient energy, costly repairs, and significant financial losses. Thereby, preventing the unplanned outage of the power transformer is still challenging for

the power utilities to maintain the availability and reliability of assets.

Oil-immersed power transformers are the most widespread type of power transformer that power utilities use in their power grid. The operation of this transformer type appears to involve more than nine gases dissolved in its insulating oil including methane, acetylene, hydrogen, ethane, ethylene, carbon dioxide, carbon monoxide, oxygen, and nitrogen [1]. These gases are detected by using chromatographic analyses of dissolved gas in

insulating oil, also known as dissolved gas analysis (DGA) [2]. The DGA method expresses gas concentration in microliter per liter ( $\mu\text{l/l}$ ) or part per million (ppm). Many power utilities use DGA techniques to investigate potential faults in the transformers. The existing fault interpretation methods based on the DGA consist of the Roger ratio method (RRM) [3], Doernenburg ratio method (DRM) [4], IEC 60599 ratio method (IEC) [5], Duval triangle method (DTM) [6], Duval pentagon method (DPM) [7], and Mansour pentagon method (MPM) [8]. These traditional techniques are classified into two types: the graphical method and the key gas ratio method. The graphical methods use fault boundary zones in graphics that are divided into each fault type zone for interpreting DGA. While the key gas ratio methods use the correlative limitations of gas ratios to identify fault types. All conventional methods have certain drawbacks in terms of accuracy and uncertainty for transformer fault type identification.

Nowadays, artificial intelligence (AI) has more influence in developing and solving problems for DGA interpretation. The AI models that are applied for DGA interpretations can be divided into three main types: supervised learning (SL), unsupervised learning (UL), and reinforcement learning (RL). The SL consists of the Artificial Neural Network (ANN) [9-11], Adaptive Neuro-Fuzzy Interference System (ANFIS) [12-14], Long Short-Term Memory (LSTM) [15-17], Support Vector Machine (SVM) [18-20], etc. These AI types require many DGA samples data with reliable fault labels to use training AI model for high accuracy in prediction. The UL model includes the Fuzzy C-Mean (FCM) [21, 22], Self-Organizing Map (SOM) [23], Density-Based Spatial Clustering of Applications with Noise (DBSCAN) [24], etc. These UL models require large amount of DGA samples to make a cluster of fault types without using the labeled actual fault in the training model. The RL is the newest AI type which does not require big data and actual fault labels in the training model at all. This AI model learns by accumulating knowledge, which mimics a human brain. The previous research [25] adopted CAI model to diagnose transformer faults based on three ratios of the DRM. This research used 117 DGA data samples for learning and validating CAI. The fault was classified into three types: arcing, thermal decomposition, and partial discharge. The result comparison showed that CAI had an accuracy of 98.3%, compared to 94.02% of the Fuzzy Inference System (FIS), and 78.6% of the ANN. Even though this approach's accuracy was high, there were some errors in the data input with DRM. This problem was solved by refining the "not significant" conditions in DRM [26] which used the same learning data set as previous research and found that the performance of CAI had decreased from the previous research. It seems the number of ratios and the ratio's vector limits have affected the performance of the diagnosis fault.

In conclusion, the existing fault diagnostic techniques are still being developed to achieve high accuracy for fault identification. The traditional methods are easy interpretation methods, but the results weren't produce the correctly accepted. The SL models mentioned above have directly and indirectly improved fault prediction accuracy by solving parameters in training data sets. However, the big problem with these AI methods is contained in the labeled fault of the training data set, while the UL approaches can remove the unreliable labeled data problem in the learning data set. On the other hand, these AI methods require big data to make partition fault groups. The new AI approach model is interesting for its ability to generate capable knowledge by itself. Nonetheless, the feature extraction data is still a necessary process in the CAI models. The previous research improved the

data features of the input by using three gas ratios of the DRM, and the result showed that the accuracy decreased. Therefore, the appropriate feature approach can develop the CAI model to achieve high performance.

This paper presents the CAI model based on the new ratio in order to increase information perception and the ability of fault type classification. This paper's major contributions are as follows:

- The proposed CAI learns without using actual fault labels.
- It does not require a large learning data set to produce a highly accurate model.
- It can provide a clear faults explanation to use for determining the maintenance plan.
- It can also apply to implementing faults in the DGA online monitoring system.

## 2.0 TRANSFORMER FAULT INTERPRETATION USING THE DGA METHOD

### 2.1 Transformer fault definition

Transformer faults are typically classified as either thermal or electrical. The IEEE Std C57.104-2019 represents the six basic fault types that are described in Figure 1 and clearly explained in Table 1. Thermal faults include high-heating fault (T3), medium-heating fault (T2), and low-heating fault (T1). Besides that, the thermal fault can be classified into sub-type such as stray gassing (S), overheating of paper or insulating oil (O), and possible carbonization of paper (C). An electrical fault consists of arcing (D2), partial discharge (PD), and low energy discharge (D1). These fault types can be investigated by using the combustible gas volume, as explained in Table 2, that is dissolved in the insulating oil. The fault interpretation techniques are introduced in the next section.

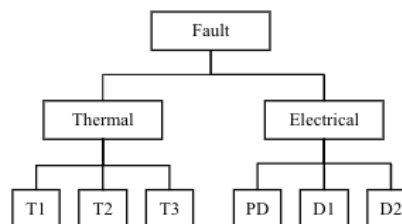


Figure 1 Basic fault type classification

Table 1 Basic fault abbreviations [27]

Fault type	Labels	Descriptions
Electrical	PD	Partial discharges
	D1	Low discharges
	D2	Arcing
Thermal	T1	Low-heating less than 300°C
	T2	Medium-heating between 300°C to 700°C
	T3	High-heating above 700°C

Table 2 Abbreviation for five combustible gases that dissolve in oil

Symbols	Descriptions
$H_2$	Hydrogen
$CH_4$	Methane
$C_2H_2$	Acetylene
$C_2H_4$	Ethylene
$C_2H_6$	Ethane

### 2.2 Conventional Fault Interpretation Methods

The conventional interpretation methods represented in this paper are classified into the gas ratio methods and the graphical methods. The gas ratio includes the IEC, RRM, and DRM. The graphic method includes DTM and DPM. All key gas ratio methods that are represented to identify fault type by matching gas ratio with fault limitation are introduced in Table 3, Table 4, and Table 5 for DRM, RRM, and IEC, respectively. The graphical methods identify fault types by indicating faults in boundary fault zones that are designed as shown in Figure 2 and Figure 3 for DTM and DPM, respectively.

**Table 3** Fault interpretation by DRM [27]

Fault types	Doernenburg ratios			
	$\frac{C_2H_2}{C_2H_4}$	$\frac{CH_4}{H_2}$	$\frac{C_2H_2}{CH_4}$	$\frac{C_2H_6}{C_2H_2}$
	Thermal faults	<0.75	>0.1	<0.3
Energy discharge	>0.75	<0.1	>0.3	<0.4
Partial discharge	Not significant	<0.1	<0.3	>0.4

**Table 4** Fault interpretation by RRM [27]

Fault types	Roger ratios		
	$\frac{C_2H_2}{C_2H_4}$	$\frac{CH_4}{H_2}$	$\frac{C_2H_4}{C_2H_6}$
	No fault	<0.1	0.1 – 1.0
Low energy discharge (PD, D1)	<0.1	<0.1	<1.0
Arcing (D2)	0.1 – 3.0	0.1 – 1.0	>3.0
Heating fault (T1)	<0.1	0.1 – 1.0	1.0 – 3.0
Heating fault 300°C -700°C (T2)	<0.1	>1.0	1.0 – 3.0
Heating fault >700°C (T3)	<0.1	>1.0	>3.0

**Table 5** Fault interpretation by IEC [28]

Fault types	IEC60599 ratios		
	$\frac{C_2H_2}{C_2H_4}$	$\frac{CH_4}{H_2}$	$\frac{C_2H_4}{C_2H_6}$
	Partial discharges (PD)	-	<0.1
Low energy discharges (D1)	>1.0	0.1 – 0.5	>1.0
Arcing (D2)	0.6 – 2.5	0.1 – 1.0	>2.0
Heating fault (T1)	-	>1.0	<1.0
Heating fault 300°C -700°C (T2)	<0.1	>1.0	1.0 – 4.0
Heating fault >700°C (T3)	<0.2	>1.0	>4.0

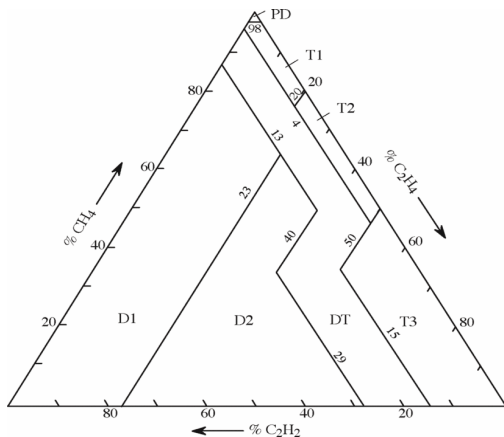


**Figure 2** Fault diagnosis by DTM [6]

### 3.0 THE PROPOSED METHOD FOR TRANSFORMER FAULT DIAGNOSIS

#### 3.1 Cognitive artificial intelligence principle

The CAI model is developed to solve problems by using the Knowledge Growing System (KGS) principle. The structure of CAI shown in Figure 4 can be divided into two main sections: the information section and the knowledge section. In the first section, the information is received by the sensors, which then inferencing-fusion information to produce new knowledge and consider it in terms of Degree of Certainty (DOC). If DOC is satisfied with new information, it will send it into the knowledge section. In this section, the newly acquired knowledge will be inferencing-fusion from the knowledge base and considered with the system's DOC. If the system's DOC is satisfied, the new knowledge will become the ultimate knowledge.

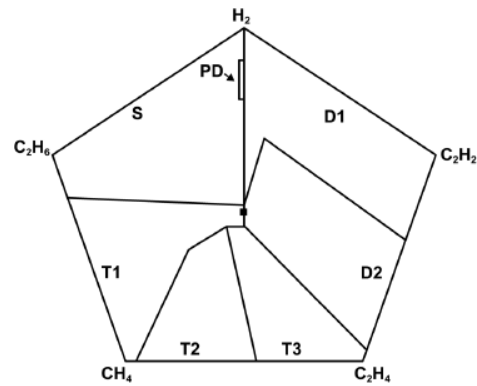


**Figure 3** Fault diagnosis by DPM [7]

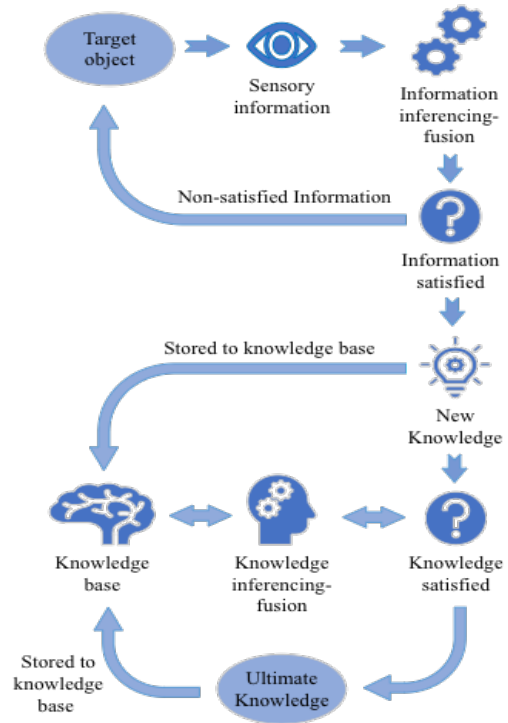


**Figure 4** The structure of KGS [29]

The information-fusion process is the main component of the CAI model, which mimics how the human brain processes information. To obtain new information, multi-source data was analyzed. The A3S information-inferencing fusion algorithm was developed in 2008 by Arwin-Adang-Aciek-Sembiring [29]. This algorithm was developed by combining the maximum a posteriori (MAP) principle, the Bayesian inference method (BIM), and the linear opinion pool (LOP) to generate the decision-making. The A3S algorithm is based on an assignment of the maximum score of the total sum of join probabilities (MSJP) method. The comprehensive conditional events of each hypothesis are fused by (1).

$$P(H_j|S_i) = \sum_n^{i=1} \left( \frac{P(S_j|H_i)P(H_j)}{\sum_{k=1}^m P(S_j|H_k)P(H_k)} \right) \quad (1)$$

where  $P(H_j|S_i)$  is the probability of the hypothesis  $H_j$  given  $S_i$ ,  $P(S_j|H_i)$  is the probability of the hypothesis  $S_i$  given  $H_j$ ,  $P(H_j)$  is the probability of the hypothesis  $H_j$ ,  $\sum_{k=1}^m P(S_j|H_k)P(H_k)$  is the combination of all possible events. The Maximum a Posterior (MAP) is performed by (2).

$$P(T_1^j) = \frac{\sum_{i=1}^{\delta} P(H_j|S_i)}{\delta} \quad (2)$$

where  $P(T_1^j)$  is the new knowledge probability distribution (NKPD) at the observation time ( $\gamma_1$ ),  $\delta$  is the total number of sensors. At this point the new knowledge is defined by (3).

$$P(T_1^j)_{estimate} = \max (P(T_1^j)) \quad (3)$$

If the system does not know what the phenomenon is at the time of the first observation, it will accumulate knowledge in form of the NKPD at each observation time as time passes. The distributions  $P(T_\gamma^j) \in P(T_1^j), \dots, P(T_\Gamma^j)$  will be the inferencing-knowledge, which is determined by (4).

$$P(\theta_\gamma^j) = \begin{cases} 1, & P(T_\gamma^j) > \frac{P(T_\gamma^j)}{\lambda} \\ 0, & P(T_\gamma^j) \leq \frac{P(T_\gamma^j)}{\lambda} \end{cases} \quad (4)$$

where  $P(\theta_\gamma^j)$  is the inferencing of each distribution that is stored in the knowledge base,  $\lambda$  is the number of fused knowledges. After being implemented in (4), the obtained result will provide new knowledge probability distribution over the time (NKPD). To acquire the final knowledge, NKPD is taken to inferencing-fusion which is performed by (5).

$$P(\theta_j) = \frac{\sum_{\gamma=1}^{\Gamma} P(\theta_\gamma^j)}{\Gamma} \quad (5)$$

$$P(\theta)_{estimate} = \max (P(\theta_j)) \quad (6)$$

where  $j = 1, \dots, \lambda$ . The degree of certainty (DOC) is used to calculate the system's confidence in the phenomenon which can be computed by (7).

$$DOC = |P(\theta)_{estimate} - P(\theta_1^j)| \times 100 \quad (7)$$

where  $P(\theta_1^j)$  is the knowledge in terms of the probability value of the  $j$  best hypothesis at observation time  $\gamma_1$ . The knowledge gained through DOC will become the ultimate knowledge.

### 3.2 Step of study

The process of the proposed method that demonstrated in Figure 5 consists of three major parts: the data feature part, the information part, and the knowledge part. The initialization of the study started with the data feature extraction to find out the vector limitation of the key gas ratio which used to be the information sensory in the proposed CAI. After that, the learning or testing process of the CAI model is performed in the information and knowledge parts. The clear explanation for each part is as follows:

#### 3.2.1 Data Feature Part

The data collected with labeled faults within six basic fault types is used to extract feature of each transformer fault phenomenon. At first, the key gas ratios are established and then calculated. The obtained gas ratios are studied in terms of the distribution value of gas ratios and the vector limitation of the gas ratio is presented based on the empirical study. In this research, the ten gas ratios ( $R_1, R_2, \dots, R_{10}$ ) are presented as the new key gas ratios. The new approach ratios are used to explain the correlation of five gases that occurred in the phenomenon of faults. The new proposed ratios are computed by:

$$R_1 = \frac{CH_4}{H_2} \quad (8)$$

$$R_2 = \frac{C_2H_6}{H_2} \quad (9)$$

$$R_3 = \frac{C_2H_4}{H_2} \quad (10)$$

$$R_4 = \frac{C_2H_2}{H_2} \quad (11)$$

$$R_5 = \frac{C_2H_6}{CH_4} \quad (12)$$

$$R_6 = \frac{C_2H_4}{CH_4} \quad (13)$$

$$R_7 = \frac{C_2H_2}{CH_4} \quad (14)$$

$$R_8 = \frac{C_2H_4}{C_2H_6} \quad (15)$$

$$R_9 = \frac{C_2H_2}{C_2H_6} \quad (16)$$

$$R_{10} = \frac{C_2H_2}{C_2H_4} \quad (17)$$

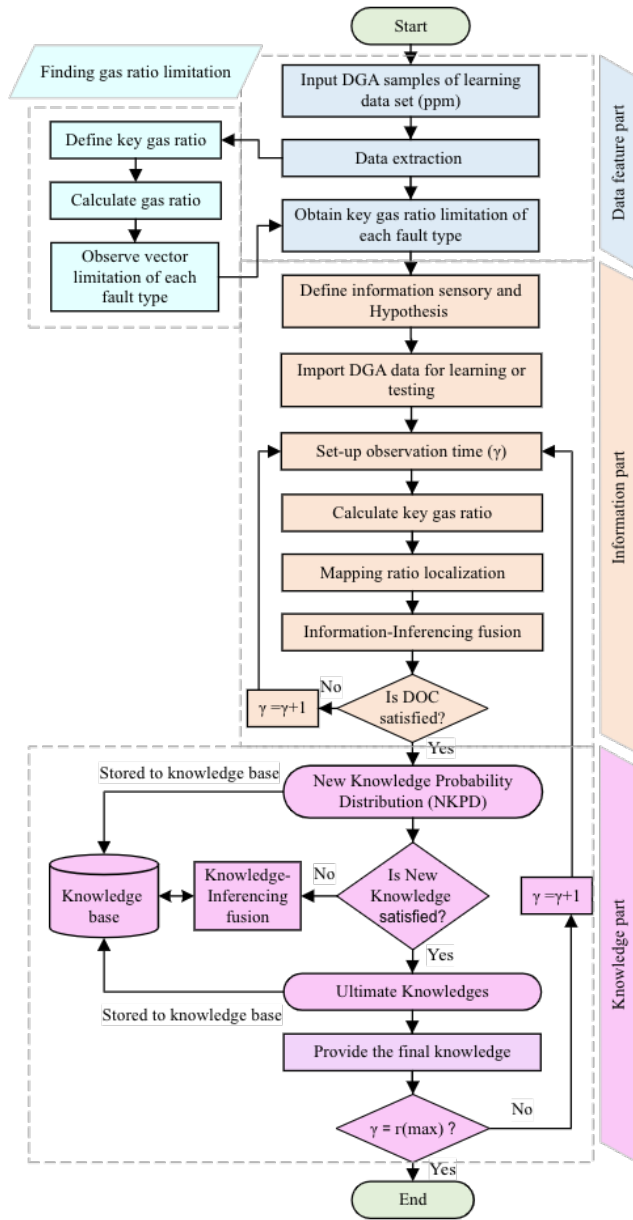


Figure 5 The proposed method flowchart

### 3.2.2 Information part

The information sensors ( $S_i$ ) and hypothesis faults ( $H_j$ ) are defined as the receiving parts and reactive parts in the CAI structure. The concentration value of the five key gases, that through the ratio method ( $R_i$ ) is transformed into information by mapping with the hypothesis fault limitation ( $L_i^j$ ) and given information knowledge by the inferencing-fusion process. The learning or testing observation time ( $\gamma$ ) is performed by setting up from the first observation  $\gamma = 1$  until  $\gamma = \Gamma_{max}$ , to simplify performance information. The information for each observation time can be obtained by (18), which result is shown in Table 6.

$$S_i^j = \begin{cases} 1, & R_i \in L_i^j \\ 0, & R_i \notin L_i^j \end{cases} \quad (18)$$

where  $S_i^j$  is the information sensor of  $R_i$  given by  $L_i^j$ . After that, the observation matrix normalized is created by comprising the inferencing-fusion method in (1) derived from the grouped localized matrix in Table 6. The observation normalized will be arrayed as in Table 7.

Table 6 Mapping ratio localization

Observation time	Ratio ( $R_i$ )	Vector limitation ( $L_j$ )			
		$L_1$	$L_2$	...	$L_m$
$\gamma$	$R_1$	$S_1^1$	$S_1^2$	...	$S_1^m$
	$R_2$	$S_2^1$	$S_2^2$	...	$S_2^m$
	...	...	...	...	...
	$R_n$	$S_n^1$	$S_n^2$	...	$S_n^m$

Table 7 Observation time matrix

Observation time	Sensor ( $S_i$ )	Hypothesis fault ( $H_j$ )			
		$H_1$	$H_2$	...	$H_m$
$\gamma$	$S_1$	$P((H_1 S_1))$	$P((H_2 S_1))$	...	$P((H_m S_1))$
	$S_2$	$P((H_1 S_2))$	$P((H_2 S_2))$	...	$P((H_m S_2))$
	...	...	...	...	...
	$S_n$	$P((H_1 S_n))$	$P((H_2 S_n))$	...	$P((H_m S_n))$

The information-inferencing is then combined by using (2) to produce the new information. If the DOC is satisfied, the new information will become the new knowledge probability distribution (NKPD). The acquired NKPD that is derived from interactive observation time will be arrayed as in Table 8.

Table 8 NKPD's matrix

Observation time ( $\gamma$ )	Hypothesis fault ( $H_j$ )			
	$H_1$	$H_2$	...	$H_m$
$\gamma_1$	$P(T_1^1)$	$P(T_1^2)$	...	$P(T_1^m)$
$\gamma_2$	$P(T_2^1)$	$P(T_2^2)$	...	$P(T_2^m)$
...	...	...	...	...
$\gamma_{max}$	$P(T_{\gamma_{max}}^1)$	$P(T_{\gamma_{max}}^2)$	...	$P(T_{\gamma_{max}}^m)$

### 3.2.3 Knowledge part

The obtained NKPD derived from the information part will be accumulated and carried out to fuse with the previous NKPD in the knowledge base, namely new knowledge over the time (NKPD) by using (5) to acquire the system's DOC from time to time. After fused knowledge, the ultimate knowledge can be obtained by using (6). The obtained NKPD will be arrayed as in Table 9. The ultimate knowledge obtained after the system's DOC is satisfied, it will be the best knowledge for the current observation time.

**Table 9** The distribution of NKPD

Stored knowledge	Hypothesis fault ( $H_j$ )			
	$H_1$	$H_2$	...	$H_m$
NKPD at $\Gamma_1$	$P(\theta_{\Gamma_1}^1)$	$P(\theta_{\Gamma_1}^2)$	...	$P(\theta_{\Gamma_1}^m)$
NKPD at $\Gamma_1$	$P(\theta_{\Gamma_1}^1)$	$P(\theta_{\Gamma_2}^2)$	...	$P(\theta_{\Gamma_2}^m)$
...	...	...	...	...
NKPD at $\Gamma_{max}$	$P(\theta_{\Gamma_{max}}^1)$	$P(\theta_{\Gamma_{max}}^2)$	...	$P(\theta_{\Gamma_{max}}^m)$

**4.0 RESULTS**

The proposed CAI model was verified with the new proposed key gas ratio limitations in Table 14 that are obtained by the fault feature extraction in the feature extraction section.

**4.1 Feature extraction**

The 941 DGA samples are derived from the IEC TC10 data set [30] and the other 45 previously published literature that is summarized in Table 11. These DGA samples consist of the  $CH_4$ ,  $C_2H_4$ ,  $C_2H_6$ ,  $C_2H_2$ , and  $H_2$ , which are defined actual faults within six basic fault labels (T1, T2, T3, PD, D1, and D2) and also include unit normal state or no fault (NF). This data set is used to feature extraction and learning processes in the proposed method. After implementing the proposed gas ratio, the gas ratio distribution value of the fault phenomenon is demonstrated as shown in Figure 9. The gas ratios are presented as an x-axis and the value of the gas ratios is expressed in the y-axis. The observation results can be divided into sixteen fault zones, as well as shown in Table 10. The gradient zones between two or three faults are created to explain the fault phenomenon and divided into three main parts: thermal fault, electrical fault, and mixed fault. The proposed fault definitions are described as follows:

- T1,T2,T3 is the thermal gradient fault.
- T1,T2 is the low-heating and medium-heating fault.
- T2,T3 is the medium-heating and high-heating fault.
- PD,T1 is the partial discharge and low-heating fault.
- PD,D1,D2 is the electrical gradient fault.
- D1,D2 is the low-discharge and aging
- D1,T2 is the mixed fault between the low-discharge and medium-heating fault.
- D2,T3 is the mixed fault between the arcing and high-heating fault.

These gradient faults might be defined as either. In order to require the maintenance task based on the proposed fault identification, there are four categories of work following: re-sampling, increase sampling, monitoring, and inspection. The explanation of the suggested works is below:

- Re-sampling: shall be yearly taken DGA.
- Increase sampling: shall be quarterly taken DGA.
- Monitoring: shall be weekly or monthly taken DGA to attend to the rate of gases that occurred.
- Inspection: shall be daily taken DGA to attend rate of gases that occurred and inspection on-site.

The ratio limits of the proposed method in Table 14 can be described by the phenomenon’s fault, which occurred in the power transformer, as following: the  $R_1$  is used as the key ratio to classify the PD fault from other faults. The  $R_2$  and  $R_{10}$  are used to divide the electrical and thermal fault. The  $R_2, R_3, R_4, R_6,$  and  $R_8$  are selected to separate within the overheating fault type. Beside that, the  $R_2, R_3, R_8,$  and  $R_{10}$  are carried out to split the electrical fault types. The rest are directly and indirectly relevant to separate faults in the proposed method.

**Table 10** Fault labeled in the proposed method

Electrical fault					Mixed fault
<b>Inspection</b>	D2	PD,D1,D2	D1,D2	D2	<b>Thermal fault</b>
<b>Monitoring</b>	D1	PD,D1	D1	T2, T3	
<b>Increase sampling</b>	PD	PD	T1	T1,T2, T3	
<b>Re-sampling</b>	NF	T1	T1	T2	
				T3	
	<b>Re-sampling</b>	<b>Increase sampling</b>	<b>Monitoring</b>	<b>Inspection</b>	

**4.2 The learning result of the proposed CAI model**

By using the learning data set to accumulate knowledge for the proposed CAI. The obtained knowledge from each observation time was stored in the knowledge base and then taken into consideration in the next observation time in terms of the system’s DOC, as shown in Figure 6. At first, the CAI might be given the incorrect decision since the system’s DOC had some collapsed points that occurred from the number of fused knowledge that was not contained enough. After figuring out the collapsed points, the system’s DOC can be significantly separated from each other which means the CAI has perceived this knowledge clearly.

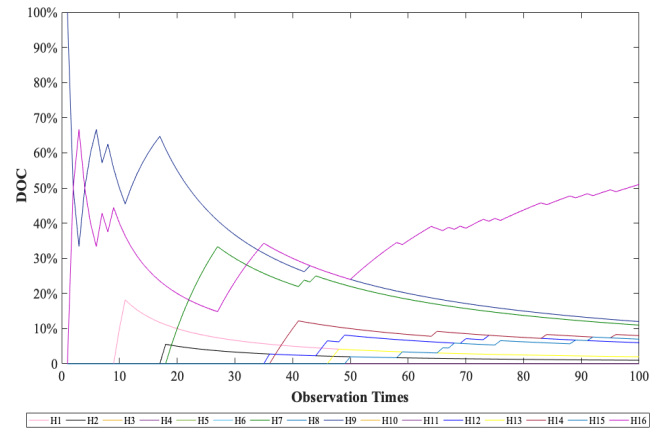


**Figure 6** System’s DOC

The fault diagnostic result of the learning data set using the proposed CAI is shown in Table 12. The result found that the highest accuracy was 98.31% for PD fault detection, followed by 85.53% of T1, 85.15% of D2, 84.96% of T3, 84.07% of D1, 63.64% of T2, and 53.47% of NF. The overall proposed diagnosis method can be the high-accuracy fault identification method.

Table 11 Data set for learning

Ref.	Year	NF	T1	T2	T3	PD	D1	D2
[31]	1999	2	0	0	5	0	0	4
[32]	2001	0	0	0	19	0	0	14
[30]	2001	0	0	0	18	9	26	48
[33]	2002	0	5	4	7	6	0	1
[9]	2004	0	0	0	3	0	0	6
[34]	2005	0	0	0	0	3	0	1
[35]	2005	9	1	3	9	0	0	18
[36]	2006	1	1	0	1	1	1	2
[37]	2007	0	0	0	2	1	0	1
[38]	2007	0	0	0	5	5	0	3
[39]	2008	1	0	0	4	0	0	4
[40]	2011	5	2	1	3	0	0	1
[41]	2012	0	0	0	6	2	2	8
[18]	2012	1	1	1	0	0	0	1
[42]	2012	0	1	0	1	1	1	1
[43]	2012	2	1	1	5	2	5	4
[10]	2012	6	2	5	6	1	1	7
[44]	2012	1	0	1	0	0	0	4
[45]	2013	1	3	0	2	0	1	2
[19]	2013	4	3	0	5	0	5	7
[46]	2014	6	2	5	6	1	1	7
[47]	2015	0	9	0	10	25	0	10
[8]	2015	0	1	1	1	1	1	1
[48]	2016	2	2	10	14	0	0	2
[49]	2016	0	2	2	2	2	2	2
[50]	2016	8	0	0	0	0	8	7
[51]	2016	3	0	0	3	0	3	3
[52]	2016	3	5	4	3	4	3	2
[53]	2016	0	2	2	2	2	2	1
[54]	2016	0	2	2	1	2	3	3
[55]	2017	0	1	1	1	1	1	1
[56]	2017	13	0	0	0	3	0	0
[57]	2019	3	3	3	2	2	4	3
[58]	2019	0	0	5	4	7	2	2
[59]	2020	21	0	0	24	16	18	23
[60]	2020	0	3	3	14	1	6	3
[61]	2021	2	0	7	6	1	0	2
[62]	2021	0	2	2	14	0	2	5
[63]	2021	0	3	3	3	5	2	4
[64]	2021	0	5	5	5	5	5	0
[65]	2021	0	1	1	1	1	1	1
[66]	2021	3	2	3	0	3	3	3
[67]	2022	0	2	1	2	2	1	2
[68]	2022	1	1	1	1	1	1	0
[69]	2022	3	0	0	3	0	0	3
[70]	2022	0	8	0	3	2	2	3
<b>Total</b>		<b>101</b>	<b>76</b>	<b>77</b>	<b>226</b>	<b>118</b>	<b>113</b>	<b>230</b>

Table 12 Confusion matrix of learning results

True prediction	Proposed CAI Diagnosis								Accuracy (%)
	NF	T1	T2	T3	PD	D1	D2		
Actual Fault	NF	54	-	1	15	15	8	8	53.47
	T1	-	65	4	2	5	-	-	85.53
	T2	-	8	49	17	3	-	-	63.64
	T3	2	2	10	191	4	1	15	84.96
	PD	2	-	-	-	116	-	-	98.31
	D1	4	-	-	1	3	95	-	84.07
	D2	4	-	-	-	-	30	196	85.15

## 5.0 VALIDATION AND COMPARISON

This section presents the proposed method validation with the testing data set as in Table 15. In order to observe and compare the result between the proposed ratio method and the gas ratio of the conventional techniques, the gas ratios in Table 3, Table 4, and Table 5 are applied to make the CAI based on the traditional ratio method which consists of the CAI-DRM, CAI-RRM, and CAI-IEC, respectively. In addition, the traditional fault interpretation methods and some of the common AI algorithms were carried out to compare the ability of fault classification in terms of thermal type and electrical type. Finally, the performance of fault identification within NF, T1, T2, T3, PD, D, and D2 were compared.

### 5.1 Testing Results Of The Proposed CAI

In this study, the testing data set was derived from two previous studies [71] and [72] as summarized in Table 15. The testing data set consists of seven labeled faults (NF, D2, D1, PD, T3, T2, and T1) and some gradient thermal faults (T1, T2) which might be selected as either. The proposed CAI model results showed that it can achieve high diagnostic accuracy as well as shown in Table 13. The confusion matrix demonstrated by the NF, T1, T2, T3, D1, and D2 was 66.67%, 93.75%, 87.50%, 100%, 92.86%, and 100%, respectively. It increased from the diagnostic accuracy of the learning process. In addition, the obtained diagnostic fault results are applied to determine the maintenance using Table 10. Finally, the maintenance determinations based on the proposed fault diagnosis method are summarized in Table 15.

Table 13 Confusion matrix of testing results

True prediction	Proposed CAI Diagnosis							Accuracy (%)	
	NF	T1	T2	T3	PD	D1	D2		
Actual Fault	NF	4	-	-	1	-	1	-	66.67
	T1	-	15	-	1	-	-	-	93.75
	T2	-	1	14	1	-	-	-	87.50
	T3	-	-	-	16	-	-	-	100.00
	PD	-	-	-	-	17	-	1	94.44
	D1	-	-	-	1	-	13	-	92.86
	D2	-	-	-	-	-	-	16	100.00

### 5.2 The Proposed CAI Comparison With The CAI Based On Conventional Ratio And Traditional Interpretation Methods

The conventional methods including DTM, DPM, DRM, IEC, RRM, and the CAI based on ratios of DRM, IEC, and RRM were taken into account to validate the diagnosis’s performance with the proposed CAI. The diagnostic result in Figure 7 showed that the performance of the proposed CAI was 92.56%, followed by CAI-DRM was 89.27%, CAI-RRM was 86.08%, DPM was 85.44%, CAI-IEC 85.33%, DTM was 84.70%, DRM was 74.39%, IEC was 71.09%, and RRM was 59.62%, respectively. For the testing data set, the fault diagnosis’s performance shown in Figure 10 demonstrated that the proposed was still the highest model, which was %, followed by CAI-DRM was %, IEC was %, CAI-IEC was %, CAI-RRM was %, DPM was %, DTM was %, DRM was %, and RRM was %, respectively. According to the results, applying the CAI model based on traditional ratios (CAI-DRM and CAI-RRM) can be greatly increased the traditional technique’s performance. The CAI-DRM that used 4 gas ratios can be produced higher performance than using 3 gas ratios of CAI-IEC and CAI-RRM. However, using 10 gas

ratios of the proposed method can be achieved the highest performance from them. As a result, the number of ratios that are used to give information knowledge into the CAI is significantly related to the diagnostic performance.

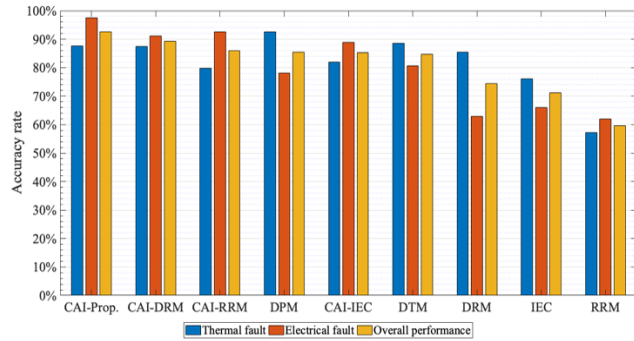


Figure 7 Illustration of the learning results comparison with conventional methods

### 5.3 The Proposed CAI Comparison With The Common AI Methods

The common AI models, including Decision Trees (DT), Support Vector Machine (SVM), Ensemble Classifiers (EC), Nearest Neighbor Classifiers (NNC), Long Short-Term Memory (LSTM), and Artificial Neuron Networks (ANN) were compared with the proposed method which used application function in MATLAB to create these AI models by using the learning data set.

The learning result in Figure 8 demonstrated the performance of the fault classification, which EC was 100%, followed by NNC was 100%, ANN was 97.45%, proposed CAI was 98.04%, DT was 95.83%, LSTM was 90.65%, and SVM was 89.80%, respectively. SL methods can produce higher diagnostic accuracy than the proposed method in the learning data set. For the testing data set, the performance of the SL methods shown in Figure 10 decreased while the proposed CAI methods succeeded highest performance which was 98.04%, followed by EC was 95.10%, DT was 94.12%, LSTM was 93.14%, SVM was 92.16%, NNC was 91.18%, and ANN was 89.22%, respectively. If considered in terms of the successful sub-type fault identification shown in Figure 11, the supervised

learning AI methods still produce high diagnostic accuracy based on comparing the fault identification's consistency, which the results showed that NNC was 99.12%, followed by EC was 98.82%, DT was 86.85%, ANN was 86.43%, proposed CAI was 79.31%, IEC was 72.46%, DPM was 57.89%, CAI-RRM was 57.05%, RRM was 56.43%, LSTM was 56.37%, DTM was 54.41%, SVM was 54.28%, and CAI-IEC was 49.07%, respectively. However, the sub-type of fault interpretation's consistency results of the testing data set shown in Figure 12 demonstrated that the proposed CAI was 90.75%, followed by IEC was 82.06%, EC was 66.75%, CAI-RRM was 65.70%, CAI-IEC was 63.45%, DT was 62.79%, RRM was 60.46%, NNC was 59.41%, LSTM was 59.06%, ANN was 58.55%, DPM was 56.55%, SVM was 50.00%, and DTM was 44.35%, respectively. According to the sub-type of fault classification's consistency results of the learning and testing data set, the deviation rate of conventional methods including DPM, DTM, RRM, and IEC are small, and the IEC method has the highest accuracy of them. The deviation rate of SL models including EC, DT, NNC, ANN, SVM, and LSTM are quite large. Since the classification ability of the SL model is decreased for interpretation faults of the testing data set. As a result, supervised learning AI methods need to update the learning to increase diagnostic accuracy. On the other hand, the CAI models can be done by itself. Therefore, the CAI model can produce a higher accuracy rate in the faults identification of the testing data set.

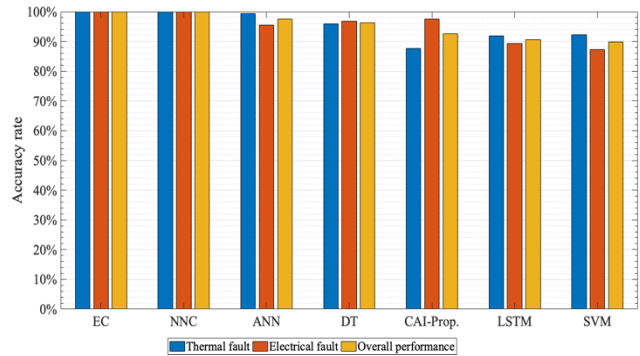


Figure 8 Illustration of the learning results comparison with supervised AI method

Table 14 The gas ratios of the proposed method

Fault label	Hypothesis	R <sub>1</sub>	R <sub>2</sub>	R <sub>3</sub>	R <sub>4</sub>	R <sub>5</sub>	R <sub>6</sub>	R <sub>7</sub>	R <sub>8</sub>	R <sub>9</sub>	R <sub>10</sub>
NF,T1	H <sub>1</sub>	>0.1	>0.4	≤0.5	<1.0	≥0	≥0	<1.0	≤0.5	<1.0	<1.0
T1	H <sub>2</sub>	>0.8	>0.01	0.5-1.25	<0.01	≥0	0.1-1.0	<0.07	>0.5	<0.3	<0.1
T1,T2	H <sub>3</sub>	1.5-5.0	0.7-1.5	>0.5	<0.15	0.1-1.0	>0.1	<0.07	0.5-4.0	<0.3	<0.1
T1,T2,T3	H <sub>4</sub>	0.1-2.0	>0.01	>0.15	0.01-1.0	>0.1	>0.1	0.01-0.6	0.5-4.0	<0.3	<0.1
T2	H <sub>5</sub>	>0.1	>1.5	>2.0	<0.4	0.1-1.5	>0.1	<0.07	0.5-2.3	<0.3	<0.1
T2,T3	H <sub>6</sub>	>0.1	>1.5	>3.5	<1.0	0.1-1.0	>0.5	<0.07	2.3-4.0	<0.3	<0.1
T3	H <sub>7</sub>	>0.1	>0.01	>1.25	≥0	>0.01	>0.5	≤1.0	>4.0	<7.0	<0.1
PD	H <sub>8</sub>	≤0.1	<0.1	<0.5	<0.01	<1.0 & int	≥0	≥0	≥0	≥0	≤0.1
PD,T1	H <sub>9</sub>	>0.1	<0.7	<0.5	<0.01	≥0	<2.0	<0.07	≥0	<0.3	<0.1
PD,D1	H <sub>10</sub>	<0.1	<1.65	<0.1	<0.7	<17	≤8.0	<20	≥0	≥0	>0.1
PD,D1,D2	H <sub>11</sub>	>0.1	<1.65	<0.1	<0.1	<6.5	<0.35	<0.25	≤3.0	≤1.0	0.1-2.0
D1	H <sub>12</sub>	>0.1	<0.45	<1.0	>0.1	>0.1	>0.1	>0.1	0.5-3.0	>0.3	0.1-2.0
D1,D2	H <sub>13</sub>	>0.1	<0.45	≥0	>0.1	≥0	>0.1	≥0	>0.5	>0.3	>2.0
D1,T2	H <sub>14</sub>	>0.1	>0.45	>0.5	>0.1	>0.1	>0.1	>0.03	0.5-3.0	>0.3	>0.1
D2	H <sub>15</sub>	>0.1	<0.45	>0.1	>0.1	≤1.0	>0.1	>0.1	>3.0	>0.3	0.1-2.0
D2,T3	H <sub>16</sub>	>0.1	>0.45	>0.5	>0.1	>0.1	>0.5	>0.4	>3.0	≥.01	>0.1

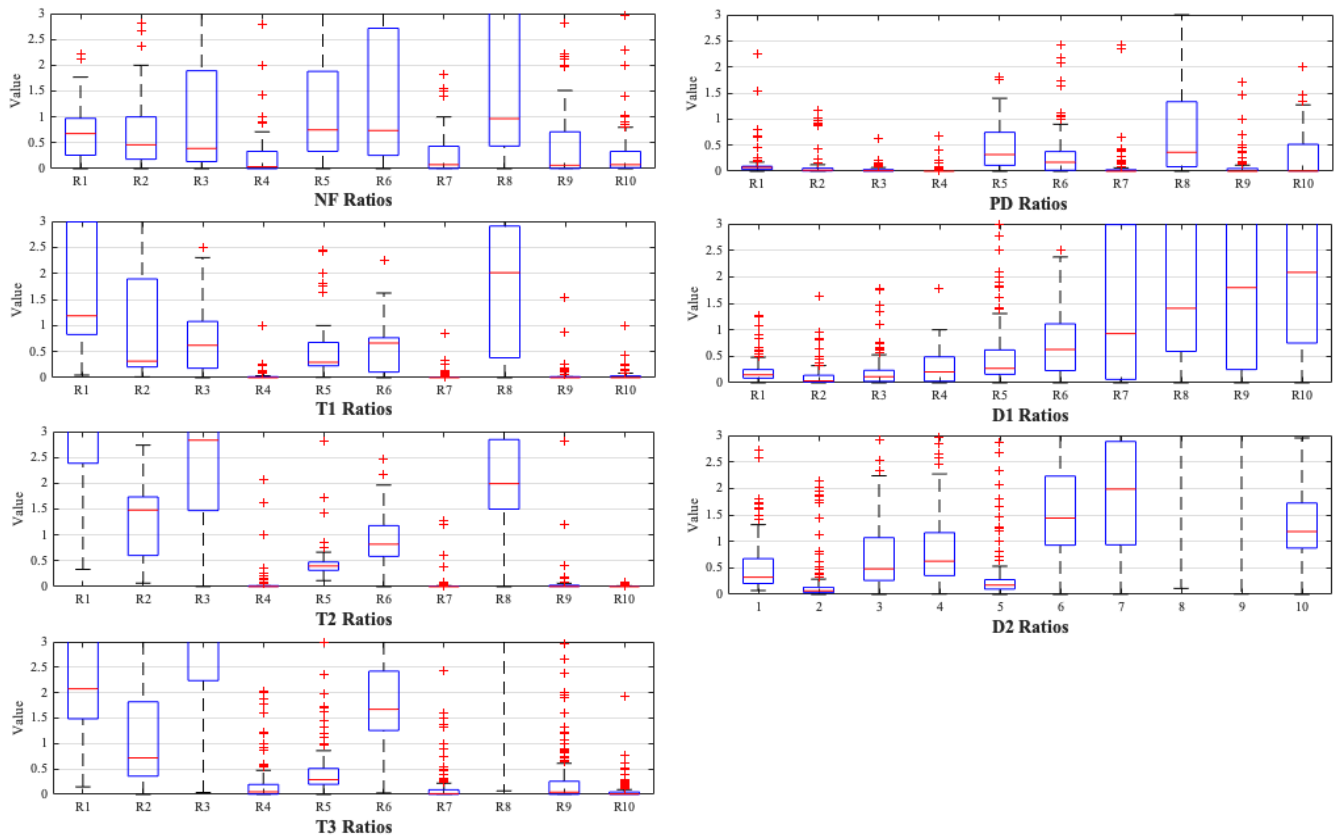


Figure 9 The distribution of basic fault labels demonstrated by 10 gas ratios

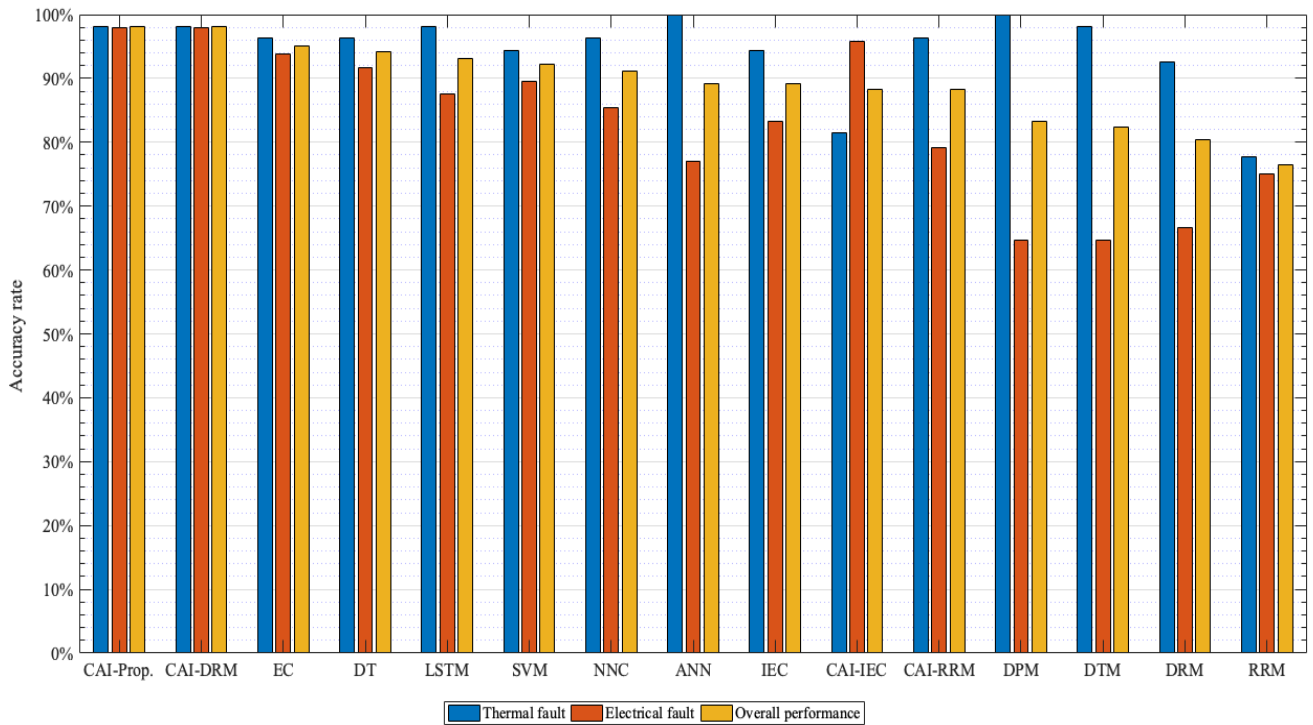


Figure 10 The performance of testing results

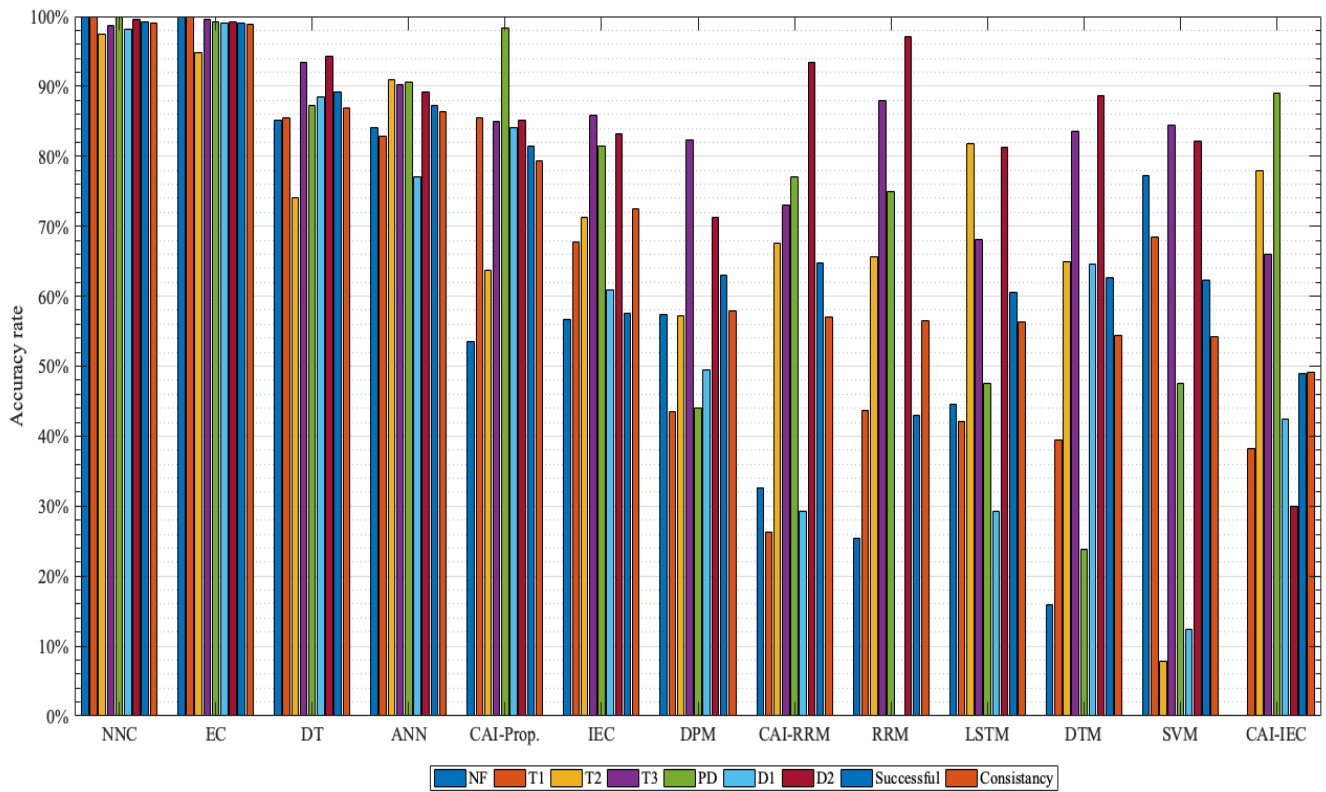


Figure 11 Illustration of learning results comparison for sub-types diagnosis

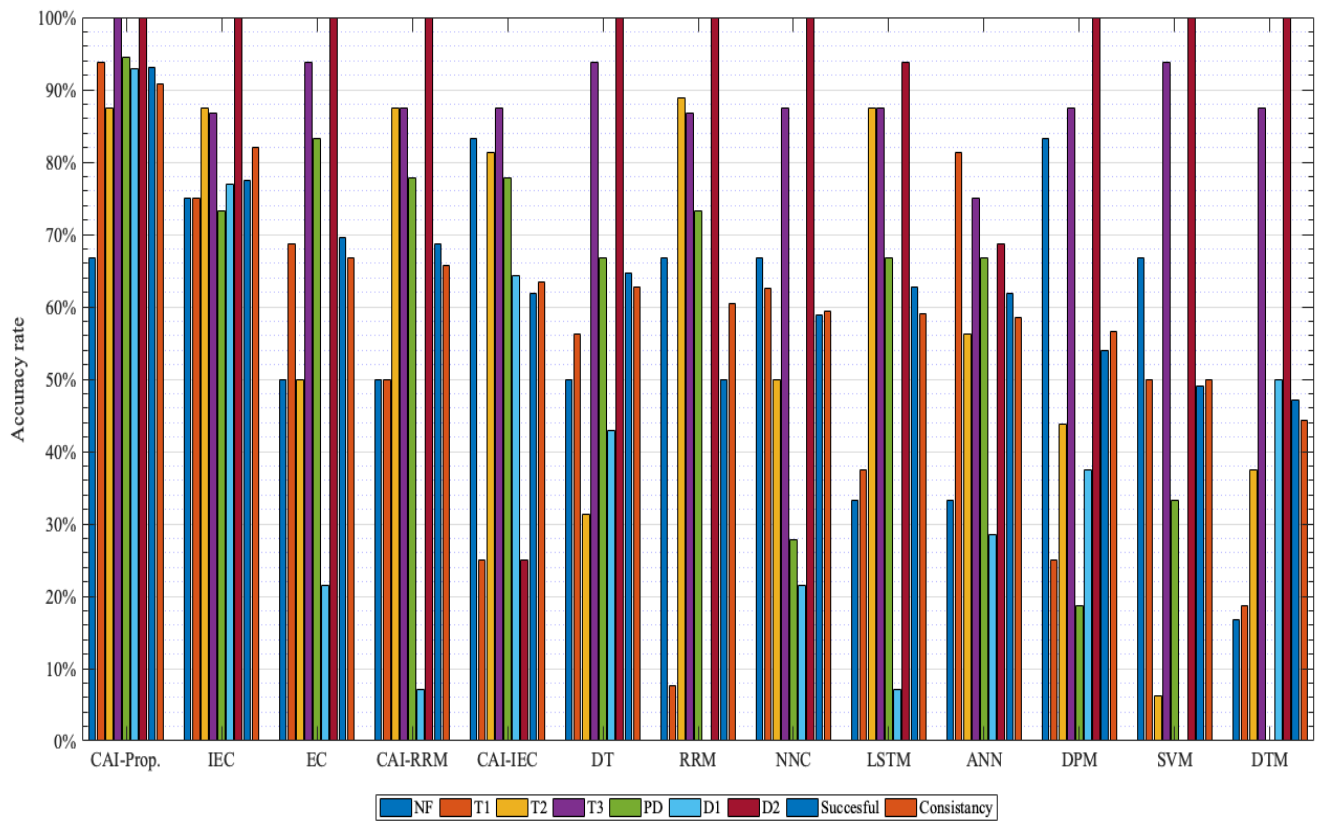


Figure 12 Illustration of testing results comparison for sub-types diagnosis

Table 15 The testing results

Ref.	H <sub>2</sub> (μl/l)	CH <sub>4</sub> (μl/l)	C <sub>2</sub> H <sub>6</sub> (μl/l)	C <sub>2</sub> H <sub>4</sub> (μl/l)	C <sub>2</sub> H <sub>2</sub> (μl/l)	Actual Fault	Proposed Method	Suggested work	Ref.	H <sub>2</sub> (μl/l)	CH <sub>4</sub> (μl/l)	C <sub>2</sub> H <sub>6</sub> (μl/l)	C <sub>2</sub> H <sub>4</sub> (μl/l)	C <sub>2</sub> H <sub>2</sub> (μl/l)	Actual Fault	Proposed Method	Suggested work
[71]	1198	3.2	1.4	3.2	0.5	D1	PD,D1	Inc.	[71]	47	120	90	198	3	T2	T2	Mon.
[71]	67.8	8.89	1.88	12.67	36.2	D1	D1,D2	Mon.	[71]	20.37	59.79	45.24	80.49	0	T2	T2	Mon.
[71]	549	121.3	25.5	31.9	198.5	D1	D1,D2	Mon.	[71]	135.65	278.53	58.86	492	2.95	T3	T3	Ins.
[71]	45	11	2.7	12.74	28.5	D1	D1,D2	Mon.	[71]	156	240	54	399	0.98	T3	T3	Ins.
[71]	101.72	27.65	7.13	16.92	53.87	D1	D1,D2	Mon.	[71]	165.62	240.95	61.32	514.53	13.53	T3	T3	Ins.
[71]	14.2	4	1.4	1.5	9.51	D1	D1,D2	Mon.	[71]	35.1	50.6	16.1	93	1.1	T3	T3	Ins.
[71]	65.2	20	3.9	8.13	25.1	D1	D1,D2	Mon.	[71]	135.88	362.42	125.22	826.65	3.74	T3	T3	Ins.
[71]	9	3.9	0.8	4	13	D1	D1,D2	Mon.	[71]	68	99.2	35.9	202.9	0	T3	T3	Ins.
[71]	30.1	17.1	2.2	5.5	30.1	D1	D1,D2	Mon.	[71]	63	149.6	57.5	276	0	T3	T3	Ins.
[71]	4.1	3.5	0.68	1.2	5.2	D1	D1,D2	Mon.	[71]	236	410.2	159	817.3	3.5	T3	T3	Ins.
[71]	75.5	30.2	2.33	30.3	18.2	D2	D2	Ins.	[71]	164	244	103	497	8.3	T3	T3	Ins.
[71]	145.88	40.65	9.37	34.02	59.71	D2	D2	Ins.	[71]	30	25.5	31.5	93	1.8	T3	T1,T2,T3	Ins.
[71]	195.7	58	16.4	91.6	96.9	D2	D2	Ins.	[72]	54	7	7.4	8.6	5.4	D1	D1	Mon.
[71]	57	15	3.1	23	25.3	D2	D2	Ins.	[72]	345	112.25	27.5	51.5	58.75	D1	D1	Mon.
[71]	755	229	32	404	460	D2	D2	Ins.	[72]	115.9	75	14.7	25.3	6.8	D1	PD,D1,D2	Mon.
[71]	475.3	195.8	32.6	187.3	221.2	D2	D2	Ins.	[72]	78	161	86	353	10	D1	T3	Ins.
[71]	56	10	1.3	13.5	17.6	D2	D2	Ins.	[72]	673.6	423.5	77.5	988.9	344.4	D2	D2	Ins.
[71]	531	111.9	22.7	122.5	169	D2	D2	Ins.	[72]	1678	652.9	80.7	1005.9	419.1	D2	D2	Ins.
[71]	65	26.1	10.1	41.6	57.8	D2	D2	Ins.	[72]	60	40	6.9	110	70	D2	D2	Ins.
[71]	1027	185	17	271	399	D2	D2	Ins.	[72]	46	37.2	8.3	107	71.9	D2	D2	Ins.
[71]	1198	3.2	1.4	3.2	0.5	PD	PD,D1	Inc.	[72]	200	48	14	117	131	D2	D2	Ins.
[71]	2587	7.88	4.7	1.4	0	PD	PD	Inc.	[72]	217.5	40	4.9	51.8	67.5	D2	D2	Ins.
[71]	485	35	29	6	0	PD	PD	Inc.	[72]	220	340	42	480	14	NF	T3	Ins.
[71]	195.9	14.5	11.6	2.4	0	PD	PD	Inc.	[72]	80	10	4	1.5	0	NF	PD,T1	Inc.
[71]	625	49	9	7	0.6	PD	PD	Inc.	[72]	7.5	5.7	3.4	2.6	3.2	NF	D1	Mon.
[71]	85.87	7.01	4.49	2.64	0	PD	PD	Inc.	[72]	30	110	137	52	22.3	NF	NF,T1	Res.
[71]	420	37.3	14.9	30	0.2	PD	PD	Inc.	[72]	14.67	3.68	10.54	2.71	0.2	NF	NF,T1	Res.
[71]	1309	124	113	6	0	PD	PD	Inc.	[72]	46.13	11.57	33.14	8.52	0.63	NF	NF,T1	Res.
[71]	102	108	70	41	0	PD	PD,T1	Inc.	[72]	2587.2	7.882	4.704	1.4	0	PD	PD	Inc.
[71]	83.26	45.32	18.1	36.45	0.26	PD	PD,T1	Inc.	[72]	1565	93	34	47	0	PD	PD	Inc.
[71]	60	60	16	40	0.3	T1	T1	Inc.	[72]	980	73	58	12	0	PD	PD	Inc.
[71]	46	98	26.3	41.3	0	T1	T1	Inc.	[72]	980	73	58	12	0	PD	PD	Inc.
[71]	120	120	33	84	0.55	T1	T1	Inc.	[72]	650	53	34	20	0	PD	PD	Inc.
[71]	110.4	112	32.5	80.8	0	T1	T1	Inc.	[72]	550	53	34	20	0	PD	PD	Inc.
[71]	143.2	123	38	75	0	T1	T1	Inc.	[72]	565	93	34	47	0	PD	PD,T1	Inc.
[71]	97	110	34	85	0	T1	T1	Inc.	[72]	24.32	16.36	1.67	30.18	27.47	PD	D2	Ins.
[71]	33	29	9	12	0	T1	PD,T1	Inc.	[72]	170	320	53	520	3.2	T1,T2	T3	Ins.
[71]	87.2	73.18	27.14	56.88	0	T1	T1	Inc.	[72]	160	130	33	96	0	T1,T2	T1	Inc.
[71]	181	162	70	132	0	T1	T1	Inc.	[72]	27	90	42	63	0.2	T1,T2	T2	Mon.
[71]	29.9	24.1	34.3	92.5	0.6	T1	T1,T2,T3	Ins.	[72]	4.32	193	118	125	0	T1,T2	T2	Mon.
[71]	24	34.6	14.2	21.7	0	T2	T1	Inc.	[72]	181	262	210	528	0	T1,T2	T1,T2	Mon.
[71]	613	3240	1432	2788	0	T2	T2	Mon.	[72]	9259	8397	26782	10497	0	T1,T2	NF,T1	Res.
[71]	20	41.9	20.2	44.2	0.38	T2	T1,T2	Mon.	[72]	274	376	55	1002	17	T3	T3	Ins.
[71]	72	442	221	461	0.7	T2	T2	Mon.	[72]	56	286	96	928	7	T3	T3	Ins.
[71]	110.6	458.8	242.6	406.4	0	T2	T2	Mon.	[72]	56	285	96	928	7	T3	T3	Ins.
[71]	46.9	161.6	94.1	193.6	0.56	T2	T2	Mon.	[72]	15	12	5.3	3.2	0.2	T3	T1,T2,T3	Ins.
[71]	128	419	269.5	614.1	0.35	T2	T2	Mon.	[72]	172.9	334.1	172.9	812.5	37.7	T3	T3	Ins.
[71]	23.51	61.33	45.21	98.03	1.01	T2	T2	Mon.	[72]	25.1	411.91	320.9	1832.8	18.4	T3	T3	Ins.

Remark: Res. means re-sampling, Mon. means monitoring, Inc. means increasing, and Ins. means inspection.

## 6.0 CONCLUSIONS

In this research, Cognitive Artificial Intelligence (CAI) is adopted for power transformer diagnosis to overcome the problems in terms of multi-source input and output in fault interpretation. To increase the performance of fault identification, the proposed method used ten key gas ratios for providing information to the CAI model. The data derived from the IEC TC10 data set and more than 45 previously published literature are used to find out and define the ratio limitation that belongs to each fault phenomenon and are also used as the learning data set for the CAI model to accumulate knowledge from the inferencing-fusion information of each observation time. Besides learn from the learning data set, the proposed method was validated using the 96 DGA samples and compared performance with conventional methods and several AI methods. The result showed that the proposed CAI model has a diagnostic accuracy of 98.04% for overall performance identification compared to 88.24% of CAI-IEC, 88.24% of CAI-RRM, 98.04% of CAI-DRM, 89.22% of IEC, 76.47% of RRM, 80.39% of DRM, 83.33% of DPM, 82.35% of DTM, 94.12% of DT, 95.10% of EC, 91.18% of NNC, 92.16 of SVM, 89.22% of ANN, and 93.14% of LSTM.

In conclusion, applying the CAI model to the transformer incipient fault diagnosis as the proposed method can achieve high performance by comparing it with the several methods in this study. The ability of information inferencing and knowledge fusion in the knowledge base of the CAI has produced higher accuracy than the traditional method. Furthermore, the proposed method has the advantage of being able to perceive information knowledge from sensors and use it to create and improve knowledge on its own, which will become more intelligent because of learning from experiences without a predetermined goal or supervised learning.

However, after an on-site inspection, it should be noted that the ratio's vector limits still provide accurate information to the CAI model to further improve the more accurate diagnostic model.

## Acknowledgement

This article has been financially supported by the collaboration project between the Electricité Du Laos and the Electricity Generating Authority of Thailand from the beginning until the end of this study. The author would like to express his gratitude to all people who have directly or indirectly contributed towards the successful completion of this research.

## References

- [1] Golarz, J. 2016. Understanding dissolved gas analysis (DGA) techniques and interpretations. *2016 IEEE/PES Transmission and Distribution Conference and Exposition (T&D)*. 1-5. doi: 10.1109/TDC.2016.7519852.
- [2] ASTM D3612-02. 2009. *Standard Test Method for Analysis of Gases Dissolved in Electrical Insulating Oil by Gas Chromatography*. ASTM Standard.
- [3] Rogers, R. R. 1978. IEEE and IEC codes to interpret incipient faults in transformers, using gas in oil analysis. *IEEE transactions on electrical insulation*, 5:349-354. doi: 10.1109/TEI.1978.298141.
- [4] IEEE Std C57.104-1978. 1978. *Guide for the Detection and Determination of Generated Gases in Oil-Immersed Transformers and Their Relation to the Serviceability of the Equipment*. IEEE Standard.

- [5] IEC 60599:1999. 1999. Interpretation of the analysis of gases in transformers and other Oil filled electrical equipment's in service. IEC Standard.
- [6] Duval, M. 2008. The duval triangle for load tap changers, non-mineral oils and low temperature faults in transformers. *IEEE Electrical Insulation Magazine*, 24(6): 22-29.
- [7] Duval, M., & Lamarre, L. 2014. The duval pentagon-a new complementary tool for the interpretation of dissolved gas analysis in transformers. *IEEE Electrical Insulation Magazine*, 30(6): 9-12. doi: 10.1109/MEI.2014.6943428.
- [8] Mansour, D. E. A. 2015. Development of a new graphical technique for dissolved gas analysis in power transformers based on the five combustible gases. *IEEE Transactions on Dielectrics and Electrical Insulation*, 22(5): 2507-2512. doi: 10.1109/TDEI.2015.004999.
- [9] Sarma, D. S., & Kalyani, G. N. S. 2004. ANN approach for condition monitoring of power transformers using DGA. *2004 IEEE Region 10 Conference TENCON 2004*, 444-447. doi: 10.1109/TENCON.2004.1414803.
- [10] Seifeddine, S., Khmais, B., & Abdelkader, C. 2012. Power transformer fault diagnosis based on dissolved gas analysis by artificial neural network. *2012 first international conference on renewable energies and vehicular technology*, 230-236. doi: 10.1109/REVET.2012.6195276.
- [11] Zakaria, F., Johari, D., & Musirin, I. 2012. Artificial neural network (ANN) application in dissolved gas analysis (DGA) methods for the detection of incipient faults in oil-filled power transformer. *2012 IEEE International Conference on Control System, Computing and Engineering*, 328-332. doi: 10.1109/ICCSCE.2012.6487165.
- [12] Vani, A., & Murthy, P. S. R. C. 2014. An adaptive neuro fuzzy inference system for fault detection in transformers by analyzing dissolved gases. *2014 The 1st International Conference on Information Technology, Computer, and Electrical Engineering*, 328-333. doi: 10.1109/ICITACEE.2014.7065766.
- [13] Kari, T., Gao, W., Zhao, D., Zhang, Z., Mo, W., Wang, Y., & Luan, L. 2018. An integrated method of ANFIS and Dempster-Shafer theory for fault diagnosis of power transformer. *IEEE Transactions on Dielectrics and Electrical Insulation*, 25(1): 360-371. doi: 10.1109/TDEI.2018.006746.
- [14] Tightiz, L., Nasab, M. A., Yang, H., & Addeh, A. 2020. An intelligent system based on optimized ANFIS and association rules for power transformer fault diagnosis. *ISA transactions*, 103: 63-74. <https://doi.org/10.1016/j.isatra.2020.03.022>
- [15] Dai, J., Song, H., Sheng, G., & Jiang, X. 2018. LSTM networks for the trend prediction of gases dissolved in power transformer insulation oil. *2018 12th International conference on the properties and applications of dielectric materials (ICPADM)*, 666-669. doi: 10.1109/ICPADM.2018.8401130.
- [16] Lin, J., Su, L., Yan, Y., Sheng, G., Xie, D., & Jiang, X. 2018. Prediction method for power transformer running state based on LSTM\_DBN network. *Energies*, 11(7): 1880. <https://doi.org/10.3390/en11071880>.
- [17] Skydt, M. R., Bang, M., & Shaker, H. R. 2021. A probabilistic sequence classification approach for early fault prediction in distribution grids using long short-term memory neural networks. *Measurement*, 170: 108691. <https://doi.org/10.1016/j.measurement.2020.108691>
- [18] Bacha, K., Souahlia, S., & Gossa, M. 2012. Power transformer fault diagnosis based on dissolved gas analysis by support vector machine. *Electric power systems research*, 83(1): 73-79. <https://doi.org/10.1016/j.epsr.2011.09.012>
- [19] Mehta, A. K., Sharma, R. N., Chauhan, S., & Saho, S. 2013. Transformer diagnostics under dissolved gas analysis using Support Vector Machine. *2013 International Conference on Power, Energy and Control (ICPEC)*, 181-186. doi: 10.1109/ICPEC.2013.6527647.
- [20] Souza, F. R., & Ramachandran, B. 2016. Dissolved gas analysis to identify faults and improve reliability in transformers using support vector machines. *2016 Clemson University Power Systems Conference (PSC)*, 1-4. doi: 10.1109/PSC.2016.7462827.
- [21] Yan-Ming, M., Qian-Yun, Y., & Ding, W. R. 2020. Fault diagnosis of transformer based on W-FCM. *2020 7th International Forum on Electrical Engineering and Automation (IFEAA)*, 339-342. doi: 10.1109/IFEAA51475.2020.00077.
- [22] Li, E., Wang, L., Song, B., & Jian, S. 2018. Improved fuzzy C-means clustering for transformer fault diagnosis using dissolved gas analysis data. *Energies*, 11(9): 2344. <https://doi.org/10.3390/en11092344>.
- [23] Misbahulumunir, S., Ramachandaramurthy, V. K., & Thayyob, Y. H. M. 2020. Improved self-organizing map clustering of power transformer

- dissolved gas analysis using inputs pre-processing. *IEEE Access*, 8: 71798-71811.
- [24] Cui, W., Chu, M., Ding, C., Wang, Y., Wang, M., & Liu, L. 2021. Research on The Fault Diagnosis Method of Oil-Immersed Transformers Based on The Improved DBSCAN Algorithm. *2021 China Automation Congress (CAC)*, 5171-5176. doi: 10.1109/CAC53003.2021.9728677.
- [25] Bachri, K. O., Khayam, U., Soedjarno, B. A., Sumari, A. D. W., & Ahmad, A. S. 2019. Cognitive artificial-intelligence for doernenburg dissolved gas analysis interpretation. *Telkonnika (Telecommunication Computing Electronics and Control)*, 17(1): 268-274. <http://doi.org/10.12928/telkonnika.v17i1.11612>.
- [26] Yaqin, E. N., & Khayam, U. 2021. Improvement of Application Cognitive Artificial Intelligence based on Doernenburg Ratio Method for Dissolved Gas Analysis Interpretation. *2021 International Conference on Electrical Engineering and Informatics (ICEEI)*, 1-5. doi: 10.1109/ICEEI52609.2021.9611122.
- [27] IEEE Std C57.104-1991. 2009. Guide for the Interpretation of Gases Generated in Oil-Immersed Transformers. IEEE Standard.
- [28] IEC 60599:2015. 2015. Mineral oil-filled electrical equipment in service – Guidance on the interpretation of dissolved and free gases analysis. IEC Standard.
- [29] Sumari, A. D. W., Ahmad, A. S., Wuryandari, A. I., & Sembiring, J. 2010. Constructing brain-inspired knowledge-growing system: a review and a design concept. *2010 International Conference on Distributed Frameworks for Multimedia Applications*, 1-7.
- [30] Duval, M., & DePabla, A. 2001. Interpretation of gas-in-oil analysis using new IEC publication 60599 and IEC TC 10 databases. *IEEE Electrical Insulation Magazine*, 17(2): 31-41. doi: 10.1109/57.917529.
- [31] Zhang, G., Yasuoka, K., Ishii, S., Yang, L., & Yan, Z. 1999. Application of fuzzy equivalent matrix for fault diagnosis of oil-immersed insulation. *Proceedings of 1999 IEEE 13th International Conference on Dielectric Liquids (ICDL'99)(Cat. No. 99CH36213)*, 400-403. doi: 10.1109/ICDL.1999.798957.
- [32] Chen, A.-P., & Lin, C. C. 2001. Fuzzy approaches for fault diagnosis of transformers. *Fuzzy Sets and Systems*, 118(1): 139-151. [https://doi.org/10.1016/S0165-0114\(99\)00115-3](https://doi.org/10.1016/S0165-0114(99)00115-3)
- [33] Bin, S., Ping, Y., Yunbai, L., & Xishan, W. 2002. Study on the fault diagnosis of transformer based on the grey relational analysis. *Proceedings. International Conference on Power System Technology*, 2231-2234. doi: 10.1109/ICPST.2002.1047179.
- [34] Castro, A. R. G., & Miranda, V. 2005. Knowledge discovery in neural networks with application to transformer failure diagnosis. *IEEE Transactions on Power Systems*, 20(2): 717-724. doi: 10.1109/TPWRS.2005.846074.
- [35] Lv, G., Cheng, H., Zhai, H., & Dong, L. 2005. Fault diagnosis of power transformer based on multi-layer SVM classifier. *Electric power systems research*, 75(1): 9-15. <https://doi.org/10.1016/j.epr.2004.07.013>
- [36] Yong-Li, Z., & Lan-qin, G. 2006. Transformer fault diagnosis based on naive Bayesian classifier and SVR. *TENCON 2006-2006 IEEE Region 10 Conference*, 1-4. doi: 10.1109/TENCON.2006.343895.
- [37] Hao, X., & Cai-Xin, S. 2007. Artificial immune network classification algorithm for fault diagnosis of power transformer. *IEEE Transactions on Power Delivery*, 22(2): 930-935. doi: 10.1109/TPWRD.2007.893182.
- [38] Sun, Y. J., Zhang, S., Miao, C. X., & Li, J. M. 2007. Improved BP neural network for transformer fault diagnosis. *Journal of China University of Mining and Technology*, 17(1): 138-142.
- [39] Tang, W. H., Lu, Z., & Wu, Q. H. 2008. A bayesian network approach to power system asset management for transformer dissolved gas analysis. *2008 Third International Conference on Electric Utility Deregulation and Restructuring and Power Technologies*, 1460-1466. doi: 10.1109/DRPT.2008.4523635.
- [40] Yadaiah, N., & Ravi, N. 2011. Internal fault detection techniques for power transformers. *Applied Soft Computing*, 11(8): 5259-5269. <https://doi.org/10.1016/j.asoc.2011.05.034>.
- [41] Agrawal, S., & Chandell, A. K. 2012. Transformer incipient fault diagnosis based on probabilistic neural network. *2012 Students Conference on Engineering and Systems*, 1-5. doi: 10.1109/SCES.2012.6199110.
- [42] Mansour, D. E. A. 2015. Development of a new graphical technique for dissolved gas analysis in power transformers based on the five combustible gases. *IEEE Transactions on Dielectrics and Electrical Insulation*, 22(5): 2507-2512. doi: 10.1109/TDEI.2015.004999.
- [43] Rajabimendi, M., & Dadios, E. P. 2012. A hybrid algorithm based on neural-fuzzy system for interpretation of dissolved gas analysis in power transformers. *TENCON 2012 IEEE region 10 conference*, 1-6. doi: 10.1109/TENCON.2012.6412171.
- [44] Souahlia, S., Bacha, K., & Chaari, A. 2012. MLP neural network-based decision for power transformers fault diagnosis using an improved combination of Rogers and Doernenburg ratios DGA. *International Journal of Electrical Power & Energy Systems*, 43(1): 1346-1353. <https://doi.org/10.1016/j.ijepes.2012.05.067>.
- [45] Ghoneim, S., & Merabtine, N. 2013. Early stage transformer fault detection based on expertise method. *International Journal of Electrical Electronics and Telecommunication Engineering*, 44(2): 1289-1294.
- [46] Ibrahim, M. M., Sayed, M. M., & El-Zahab, E. A. 2014. Diagnosis of power transformer incipient faults using fuzzy logic-IEC based approach. *2014 IEEE International Energy Conference (ENERGYCON)*, 242-245. doi: 10.1109/ENERGYCON.2014.6850435.
- [47] Liu, Z. X., Song, B., Li, E. W., Mao, Y., & Wang, G. L. 2015. Study of "code absence" in the IEC three-ratio method of dissolved gas analysis. *IEEE Electrical Insulation Magazine*, 31(6): 6-12. doi: 10.1109/MEI.2015.7303257.
- [48] Gouda, O. E., Saleh, S. M., & El-Hoshy, S. H. 2016. Power transformer incipient faults diagnosis based on dissolved gas analysis. *TELKOMNIKA Indonesian J. Electr. Eng.*, 17(1): 10-16.
- [49] Taha, I. B., Ghoneim, S. S., & Zaini, H. G. 2016. A fuzzy diagnostic system for incipient transformer faults based on DGA of the insulating transformer oils. *International Review of Electrical Engineering (IREE)*, 11(3): 305-313.
- [50] Ilias, H. A., & Chai, X. R. 2016. Hybrid modified evolutionary particle swarm optimisation-time varying acceleration coefficient-artificial neural network for power transformer fault diagnosis. *Measurement*, 90: 94-102. <https://doi.org/10.1016/j.measurement.2016.04.052>.
- [51] Li, J., Zhang, Q., Wang, K., Wang, J., Zhou, T., & Zhang, Y. 2016. Optimal dissolved gas ratios selected by genetic algorithm for power transformer fault diagnosis based on support vector machine. *IEEE Transactions on Dielectrics and Electrical Insulation*, 23(2): 1198-1206. doi: 10.1109/TDEI.2015.005277.
- [52] Malik, H., & Mishra, S. 2016. Application of gene expression programming (GEP) in power transformers fault diagnosis using DGA. *IEEE Transactions on Industry Applications*, 52(6): 4556-4565. doi: 10.1109/TIA.2016.2598677.
- [53] Ngwenyama, M. K., & Gitau, M. N. 2024. Discernment of transformer oil stray gassing anomalies using machine learning classification techniques. *Scientific Reports*, 14(1): 376.
- [54] Ghoneim, S. S., & Taha, I. B. 2016. A new approach of DGA interpretation technique for transformer fault diagnosis. *International Journal of Electrical Power & Energy Systems*, 81: 265-274.
- [55] Faiz, J., & Soleimani, M. 2017. Dissolved gas analysis evaluation in electric power transformers using conventional methods a review. *IEEE Transactions on Dielectrics and Electrical Insulation*, 24(2): 1239-1248.
- [56] Peimankar, A., Weddell, S. J., Jalal, T., & Laphorn, A. C. 2017. Evolutionary multi-objective fault diagnosis of power transformers. *Swarm and Evolutionary Computation*, 36: 62-75. <https://doi.org/10.1016/j.swevo.2017.03.005>.
- [57] Mharakurwa, E. T., Nyakoe, G. N., & Akumu, A. O. 2019. Power transformer fault severity estimation based on dissolved gas analysis and energy of fault formation technique. *Journal of Electrical and Computer Engineering*, 2019(1): 9674054. <https://doi.org/10.1155/2019/9674054>.
- [58] Zeng, B., Guo, J., Zhu, W., Xiao, Z., Yuan, F., & Huang, S. 2019. A transformer fault diagnosis model based on hybrid grey wolf optimizer and LS-SVM. *Energies*, 12(21): 4170. <https://doi.org/10.3390/en12214170>
- [59] Kirkbas, A., Demircali, A., Koroglu, S., & Kizilkaya, A. 2020. Fault diagnosis of oil-immersed power transformers using common vector approach. *Electric Power Systems Research*, 184: 106346. <https://doi.org/10.1016/j.epr.2020.106346>.
- [60] Liu, Y., Song, B., Wang, L., Gao, J., & Xu, R. 2020. Power transformer fault diagnosis based on dissolved gas analysis by correlation coefficient-DBSCAN. *Applied Sciences*, 10(13): 4440. <https://doi.org/10.3390/app10134440>.
- [61] Naganathan, G. S., Senthilkumar, M., Aiswariya, S., Muthulakshmi, S., Riyasen, G. S., & Priyadharshini, M. M. 2021. WITHDRAWN: Internal

- fault diagnosis of power transformer using artificial neural network. <https://doi.org/10.1016/j.matpr.2021.02.206>.
- [62] Nanfak, A., Eke, S., Kom, C. H., Mouangue, R., & Fofana, I. 2021. Interpreting dissolved gases in transformer oil: A new method based on the analysis of labelled fault data. *IET Generation, Transmission & Distribution*, 15(21): 3032-3047. <https://doi.org/10.1049/gtd2.12239>.
- [63] Kherif, O., Benmahamed, Y., Teguair, M., Boubakeur, A., & Ghoneim, S. S. 2021. Accuracy improvement of power transformer faults diagnostic using KNN classifier with decision tree principle. *IEEE Access*, 9: 81693-81701. doi: 10.1109/ACCESS.2021.3086135.
- [64] Taha, I. B., Ibrahim, S., & Mansour, D. E. A. 2021. "Power transformer fault diagnosis based on DGA using a convolutional neural network with noise in measurements," *IEEE Access*, 9: 111162-111170.
- [65] Wang, G., Xia, G., Su, Z., Dai, Y., & Lu, L. 2021. A Fault Diagnosis Method of Power Transformer Based on Improved DDAG-SVM. *2021 IEEE 2nd China International Youth Conference on Electrical Engineering (CIYCEE)*, 1-5. doi: 10.1109/CIYCEE53554.2021.9676904.
- [66] Wu, Y., Sun, X., Zhang, Y., Zhong, X., & Cheng, L. 2021. A power transformer fault diagnosis method-based hybrid improved seagull optimization algorithm and support vector machine. *IEEE Access*, 10: 17268-17286. doi: 10.1109/ACCESS.2021.3127164.
- [67] Wu, Y., Sun, X., Dai, B., Yang, P., & Wang, Z. 2022. A transformer fault diagnosis method based on hybrid improved grey wolf optimization and least squares-support vector machine. *IET generation, transmission & distribution*, 16(10): 1950-1963. <https://doi.org/10.1049/gtd2.12405>.
- [68] Ding, C., Ding, Q., Wang, Z., & Zhou, Y. 2022. Fault diagnosis of oil-immersed transformers based on the improved sparrow search algorithm optimised support vector machine. *IET Electric Power Applications*, 16(9): 985-995. <https://doi.org/10.1049/elp2.12204>.
- [69] Feng, L., & Bo, Y. 2022. Intelligent fault diagnosis technology of power transformer based on Artificial Intelligence. *2022 IEEE 6th Information Technology and Mechatronics Engineering Conference (ITOEC)*, 1968-1971. doi: 10.1109/ITOEC53115.2022.9734331.
- [70] Yi, L., Jiang, G., Zhang, G., Yu, W., Guo, Y., & Sun, T. 2022. A fault diagnosis method of oil-immersed transformer based on improved harris hawks optimized random forest. *Journal of Electrical Engineering & Technology*, 17(4): 2527-2540.
- [71] Li, E., Wang, L., & Song, B. 2019. Fault diagnosis of power transformers with membership degree. *IEEE Access*, 7: 28791-28798. doi: 10.1109/ACCESS.2019.2902299.
- [72] Li, Z. J., Chen, W. G., Shan, J., Yang, Z. Y., & Cao, L. Y. 2022. Enhanced distributed parallel firefly algorithm based on the Taguchi method for transformer fault diagnosis. *Energies*, 15(9): 3017. <https://doi.org/10.3390/en15093017>